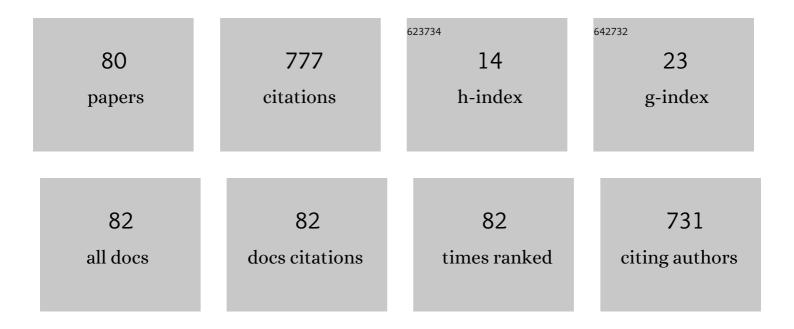
List of Publications by Year in descending order

Source: https://exaly.com/author-pdf/2652175/publications.pdf Version: 2024-02-01



#	Article	IF	CITATIONS
1	Influence of Molybdenum on the Microstructure, Mechanical Properties and Corrosion Resistance of Ti20Ta20Nb20(ZrHf)20â^²xMox (Where: x = 0, 5, 10, 15, 20) High Entropy Alloys. Materials, 2022, 15, 393.	2.9	11
2	Microstructure refinement and mechanical properties of the NiCoMnIn alloy obtained by arc melting technique from mechanically alloyed powder. Journal of Alloys and Compounds, 2021, 859, 157841.	5.5	2
3	Correlation between Microstructure and Magnetism in Ball-Milled SmCo5/α-Fe (5%wt. α-Fe) Nanocomposite Magnets. Materials, 2021, 14, 805.	2.9	5
4	Priscillagrewite-(Y), (Ca2Y)Zr2Al3O12: A new garnet of the bitikleite group from the Daba-Siwaqa area, the Hatrurim Complex, Jordan. American Mineralogist, 2021, 106, 641-649.	1.9	5
5	Structural, magnetic, and electronic properties of Ti2CrAl. Journal of Alloys and Compounds, 2021, 867, 159078.	5.5	6
6	Amorphous/crystalline Fe ₅₅ Ni ₂₀ Cu ₅ P ₁₀ Si ₅ B ₅ composite produced by two-component melt–spinning. Materials Science and Technology, 2020, 36, 982-988.	1.6	1
7	Analysis of Stainless Steel Waste Products Generated during Laser Cutting in Nitrogen Atmosphere. Metals, 2020, 10, 1572.	2.3	7
8	Microstructure and Mechanical Properties of Co-Cr-Mo-Si-Y-Zr High Entropy Alloy. Metals, 2020, 10, 1456.	2.3	4
9	Microstructure and magnetic properties of nanocrystalline Fe-Pt-based ribbons. Journal of Magnetism and Magnetic Materials, 2020, 501, 166472.	2.3	0
10	Structure of the Ni-Co-Mn-In alloy obtained by mechanical alloying and sintering. Journal of Alloys and Compounds, 2019, 801, 529-535.	5.5	14
11	Experimental and theoretical studies of Ti2MnGa. Materials Characterization, 2019, 154, 248-252.	4.4	3
12	Microstructural and magnetic characterization of Ni0.5Zn0.5Fe2O4 ferrite nanoparticles. Journal of Physics and Chemistry of Solids, 2019, 129, 1-21.	4.0	81
13	The Comparison of Magnetic Properties at Room Temperature in RCo5 (R = Y, Sm, and Gd) Nanoflakes Synthesized via Time-Staged HEBM. IEEE Transactions on Magnetics, 2019, 55, 1-4.	2.1	4
14	Evolution of frozen magnetic state in co-precipitated Zn δ Co 1â^' δ Fe 2 O 4 (0†â‰≇€ δ †â‰≇€ 1) ferrite Journal of Magnetism and Magnetic Materials, 2018, 454, 368-374.	nan <u>op</u> owd	ers. 6
15	Formation and microstructure of the amorphous/crystalline Fe55Ni20Cu5P10Si5B5 composite produced by two-component melt-spinning. Journal of Alloys and Compounds, 2018, 750, 471-478.	5.5	4
16	Microstructure and some thermomagnetic properties of amorphous Fe-(Co)-Mn-Mo-B alloys. Journal of Alloys and Compounds, 2018, 735, 253-260.	5.5	13
17	Magnetic Hardening Induced in RCo5 (R = Y, Gd, Sm) by Short HEBM. Acta Physica Polonica A, 2018, 133, 688-690.	0.5	4
18	Influence of Substitution and Milling on Structural and Magnetic Properties of Selected Sm(Ni _{1-x} Co _x) ₃ Compounds. Acta Physica Polonica A, 2018, 133, 486-488.	0.5	1

#	Article	IF	CITATIONS
19	HoFe 3 magnetic nanopowders fabricated by high energy ball milling. Materials Characterization, 2017, 126, 42-56.	4.4	5
20	Characterization of HoCo 3 nanoflakes synthesized via high energy ball– milling. Materials Chemistry and Physics, 2017, 194, 105-117.	4.0	3
21	Novel Ho(Ni 0.8 Co 0.2) 3 nanoflakes produced by high energy ball – milling. Materials Characterization, 2017, 128, 43-53.	4.4	1
22	The effects of room temperature ECAP and subsequent aging on the structure and properties of the Al-3%Mg aluminium alloy. Materials Characterization, 2017, 133, 185-195.	4.4	51
23	Gurimite, Ba3(VO4)2 and hexacelsian, BaAl2Si2O8 – two new minerals from schorlomite-rich paralava of the Hatrurim Complex, Negev Desert, Israel. Mineralogical Magazine, 2017, 81, 1009-1019.	1.4	21
24	Mechanical properties of Ni-Fe-Cu-P-B alloy produced by two component melt spinning (TCMS). Archives of Metallurgy and Materials, 2017, 62, 137-140.	0.6	0
25	Dzierżanowskite, CaCu2S2 – a new natural thiocuprate from Jabel Harmun, Judean Desert, Palestine Autonomy, Israel. Mineralogical Magazine, 2017, 81, 1073-1085.	1.4	12
26	Preparation and Magnetic Characteristics of Co _{1-δ} Zn _δ Fe ₂ O ₄ Ferrite Nanopowders. Acta Physica Polonica A, 2017, 131, 1236-1239.	0.5	3
27	Magnetic Properties and Structure of the Ni-Co-Mn-In Alloys with the Boron Addition. Acta Physica Polonica A, 2017, 131, 1240-1244.	0.5	3
28	Evolution of morphology and magnetism of Ho(Fe 0.5 Co 0.5) 3 intermetallic nanopowders synthesized by HEBM. Intermetallics, 2016, 76, 56-69.	3.9	6
29	Application of HEBM for obtaining Ho(Ni 0.5 Co 0.5) 3 nanoflakes. Materials Chemistry and Physics, 2016, 177, 299-313.	4.0	10
30	Structure and properties of AlMg alloy after combination of ECAP and post-ECAP ageing. Archives of Civil and Mechanical Engineering, 2016, 16, 325-334.	3.8	37
31	Effect of the Boron Addition on the Structure of the Ni-Mn-Co-In Alloys. Acta Physica Polonica A, 2016, 130, 1023-1025.	0.5	5
32	Influence of High Energy Milling Time on the Ti-50Ta Biomedical Alloy Structure. Acta Physica Polonica A, 2016, 130, 1033-1036.	0.5	7
33	The Microstructure and Thermal Stability of the Two-Component Melt-Spun Ni ₅₅ Fe ₂₀ Cu ₅ P ₁₀ B ₁₀ TCMS Amorphous/Amorphous Composite. Acta Physica Polonica A, 2016, 130, 927-930.	0.5	1
34	Structure of the Extruded and Thermally Treated Ni54.3Fe16.2Ga29.5Alloy. Acta Physica Polonica A, 2016, 130, 1020-1022.	0.5	0
35	Study of morphology and magnetic properties of the HoNi3 crystalline and ball-milled compound. Materials Characterization, 2015, 101, 58-70.	4.4	14
36	Rapid continuous microwave-assisted synthesis of silver nanoparticles to achieve very high productivity and full yield: from mechanistic study to optimal fabrication strategy. Journal of Nanoparticle Research, 2015, 17, 27.	1.9	31

#	Article	IF	CITATIONS
37	Microstructure, fracture, and thermal stability of Ni–Fe–Cu–P–B two-phase amorphous composite produced from the double-chamber crucible. Intermetallics, 2015, 65, 15-21.	3.9	6
38	Ultra-high coercivity of (Fe 86â^' x Nb x B 14) 0.88 Tb 0.12 bulk nanocrystalline magnets. Acta Materialia, 2015, 98, 318-326.	7.9	22
39	Microstructure and fracture surface of the two-component melt-spun amorphous/amorphous composite. Journal of Non-Crystalline Solids, 2015, 412, 49-52.	3.1	6
40	Synthesis of nanostructured Ho(Ni0.5Fe0.5)3 compound via ball-milling. Materials Characterization, 2015, 110, 145-159.	4.4	9
41	Magnetic Properties of Tb(Ni_{1-x}Fe_{x})_{3} (x=0.2, 0.6) Crystalline Compounds and Powders. Acta Physica Polonica A, 2014, 126, 180-181.	0.5	9
42	Microstructure of the Ni–Fe–Cu–P melt-spun ribbons produced from the single-chamber and from the double-chamber crucibles. Journal of Alloys and Compounds, 2014, 615, S29-S34.	5.5	17
43	Amine-stabilized small gold nanoparticles supported on AlSBA-15 as effective catalysts for aerobic glucose oxidation. Applied Catalysis A: General, 2014, 475, 203-210.	4.3	18
44	Microstructure, Phase Transformations, and Properties of Hot-Extruded Ni-Rich NiTi Shape Memory Alloy. Journal of Materials Engineering and Performance, 2014, 23, 2362-2367.	2.5	13
45	Irinarassite Ca3Sn2SiAl2O12 – new garnet from the Upper Chegem Caldera, Northern Caucasus, Kabardino-Balkaria, Russia. Mineralogical Magazine, 2013, 77, 2857-2866.	1.4	7
46	Dzhuluite, Ca3SbSnFe3+3O12, a new bitikleite-group garnet from the Upper Chegem Caldera, Northern Caucasus, Kabardino-Balkaria, Russia. European Journal of Mineralogy, 2013, 25, 231-239.	1.3	6
47	Eltyubyuite, Ca12Fe3+10Si4O32Cl6 - the Fe3+ analogue of wadalite: a new mineral from the Northern Caucasus, Kabardino-Balkaria, Russia. European Journal of Mineralogy, 2013, 25, 221-229.	1.3	10
48	Megawite, CaSnO ₃ : a new perovskite-group mineral from skarns of the Upper Chegem caldera, Kabardino-Balkaria, Northern Caucasus, Russia. Mineralogical Magazine, 2011, 75, 2563-2572.	1.4	11
49	Influence of Primary Milling on Structural and Electrical Properties of Bi4Ti3O12 Ceramics Obtained by Sintering Process. International Journal of Thermophysics, 2010, 31, 42-54.	2.1	7
50	Properties and microstructure of the (Fe, Ni)–Cu–(P, Si, B) meltâ€spun alloys. Journal of Microscopy, 2010, 237, 232-236.	1.8	15
51	Structure and Properties of the Melt-Spun Fe ₄₁ Ni ₃₉ P ₁₀ Si ₅ B ₅ Alloy Heat Treated at Elevated Temperatures. Solid State Phenomena, 2010, 163, 101-105.	0.3	Ο
52	Elbrusite-(Zr)A new uranian garnet from the Upper Chegem caldera, Kabardino-Balkaria, Northern Caucasus, Russia. American Mineralogist, 2010, 95, 1172-1181.	1.9	45
53	Bitikleite-(SnAl) and bitikleite-(ZrFe): New garnets from xenoliths of the Upper Chegem volcanic structure, Kabardino-Balkaria, Northern Caucasus, Russia. American Mineralogist, 2010, 95, 959-967.	1.9	20
54	Toturite Ca3Sn2Fe2SiO12A new mineral species of the garnet group. American Mineralogist, 2010, 95, 1305-1311.	1.9	21

#	Article	IF	CITATIONS
55	Eringaite, Ca3Sc2(SiO4)3, a new mineral of the garnet group. Mineralogical Magazine, 2010, 74, 365-373.	1.4	16
56	Nanocrystalline MgO powder materials prepared by sol-gel studied by X-ray diffraction and electron microscopy. Zeitschrift Für Kristallographie, Supplement, 2009, 2009, 255-260.	0.5	4
57	Effect of composition and heat treatment on the martensitic transformations in Co–Ni–Ga alloys. Materials Science & Engineering A: Structural Materials: Properties, Microstructure and Processing, 2008, 481-482, 330-333.	5.6	11
58	Effect of deformation on structure and mechanical behavior of polycrystalline Ni-Mn-Ga alloys. European Physical Journal: Special Topics, 2008, 158, 93-98.	2.6	1
59	The effect of γ-phase particles on microstructure and properties of Co-Ni-Ga alloys. European Physical Journal: Special Topics, 2008, 158, 155-159.	2.6	12
60	Structural Studies with the Use of XRD and Mössbauer Spectroscopy οf Bi ₅ Ti ₃ FeO ₁₅ Ceramic Powders Obtained by Mechanical Synthesis. Acta Physica Polonica A, 2008, 114, 1623-1629.	0.5	4
61	Martensitic Transformation, Structure and Magnetic Properties of Co-Ni-Ga Ferromagnetic Shape Memory Alloys. Solid State Phenomena, 2007, 130, 141-146.	0.3	2
62	Structure Analysis of Nanocrystalline MgO Aerogel Prepared by Sol-Gel Method. Solid State Phenomena, 2007, 130, 203-206.	0.3	4
63	X-ray studies on NiAl–Cr3C2–Al2O3 composite powder with nanocrystalline NiAl phase. Journal of Alloys and Compounds, 2006, 423, 112-115.	5.5	9
64	Microstructure of Ni(Cr)–TiC–Cr3C2–Cr7C3 composite powder. Journal of Materials Processing Technology, 2005, 162-163, 15-19.	6.3	14
65	Texture Analysis of Hot Rolled Ni-Mn-Ga Alloys. Solid State Phenomena, 0, 154, 133-138.	0.3	16
66	Extruded Rods with <001> Axial Texture of Polycrystalline Ni-Mn-Ga Alloys. Materials Science Forum, 0, 635, 189-194.	0.3	9
67	Structure of the Near Stoichiometric Thermally Treated Co ₂ NiGa Heusler Compounds. Solid State Phenomena, 0, 163, 131-136.	0.3	1
68	Crystallite Size Determination of MgO Nanopowder from X-Ray Diffraction Patterns Registered in GIXD Technique. Solid State Phenomena, 0, 163, 177-182.	0.3	20
69	Studies of Plastically Deformed Ni-Mn-Ga Ferromagnetic Shape Memory Alloy. Solid State Phenomena, 0, 163, 123-126.	0.3	2
70	TEM Study of Ni-Mn-Co-In Ferromagnetic Shape Memory Alloys. Solid State Phenomena, 0, 186, 271-274.	0.3	0
71	Characterization of Precipitation Process in T24 Steel after Long–Term Ageing. Solid State Phenomena, 0, 186, 296-300.	0.3	1
72	Formation and Properties of Amorphous/Crystalline Ductile Composites in Ni-Ag-P Immiscible Alloys. Solid State Phenomena, 0, 186, 216-221.	0.3	12

KRYSTIAN PRUSIK

#	Article	IF	CITATIONS
73	Rietveld Analysis of Aurivillius-Type Structure Ceramics Synthesized from Precursors Prepared by Classical and HEBM Methods. Solid State Phenomena, 0, 203-204, 319-322.	0.3	0
74	Structure and Phase Transformation in Ni-Co-Mn-In Ferromagnetic Shape Memory Alloys. Solid State Phenomena, 0, 203-204, 240-245.	0.3	1
75	Microstructural Studies of NiCoMnIn Magnetic Shape Memory Ribbons. Materials Science Forum, 0, 738-739, 436-440.	0.3	0
76	Preparation and Structural Examinations of Gd+Ni Nanocomposites. Solid State Phenomena, 0, 203-204, 276-279.	0.3	1
77	Microstructure of the Fe-Ni-P Melt-Spun Ribbons Produced from the Single-Chamber and from the Double-Chamber Crucibles. Solid State Phenomena, 0, 203-204, 361-367.	0.3	8
78	Hot Extrusion of Ni-Based Polycrystalline Ferromagnetic Shape Memory Alloys. Solid State Phenomena, 0, 203-204, 306-309.	0.3	4
79	The Nanoflower-Like Morphology and Magnetism of As-Milled Ho(Ni _{0.8} Co _{0.2}) ₃ Powders Prepared by HEBM. Solid State Phenomena, 0, 257, 76-80.	0.3	1
80	Structure Analysis of Nanocrystalline MgO Aerogel Prepared by Sol-Gel Method. Solid State Phenomena, 0, , 203-206.	0.3	1